Geophysical Research Letters

Supporting Information for

Coherent wavefield reconstruction improves event location with dense seismic arrays

Lei Li[1,2,3] and Benjamin Schwarz[4*]

1. Key Laboratory of Metallogenic Prediction of Nonferrous Metals and Geological Environment Monitoring (Central South University), Ministry of Education, 410083 Changsha, China.
2. Hunan Key Laboratory of Nonferrous Resources and Geological Hazard Exploration, 410083 Changsha, China.
3. School of Geosciences and Info-Physics, Central South University, 410083 Changsha, China.
4. GFZ German Research Centre for Geosciences, 14473 Potsdam, Germany.

Contents of this file

Other Supplementary Material for this manuscript includes the following:

Movies S1 to S5

Introduction

The text, figures and table included in this document are designed to complement and support the analysis presented in the main text.

Text S1: Generation of realistic waveform data

To generate realistic synthetic data, we use the same model parameters of event ML203 and event 24021, including the velocity model, source parameters, and station geometry, to simulate the waveforms, and then add corresponding field noise from each station to respective traces of synthetic waveforms. The noise is created and defined by the following equation (Staněk et al., 2014) :

$$Noise = \frac{A_{noise}}{mean(|A_{noise}|)} \cdot mean\left(\left|A_{synthetic}\right|\right) \cdot NL\,, \qquad \text{(S1)}$$

where A_{noise} is the noise retrieved from field waveforms on each trace at a given time window before the first arrival, $A_{synthetic}$ is the computed amplitudes for the given model parameters, NL means the level or intensity of the noise, which approximates the reversed value of the SNR. The selected noise amplitudes are extended recurrently to match the noise-free synthetic amplitudes. In this work, we select the first 400 samples of noise amplitudes from each trace to resemble the field noise and set the noise level as 0, 5, and 10, denoting them as noise-free, SNR~1, and SNR<1, respectively. The $Noise$ is then added to the original synthetic amplitudes to obtain realistic waveforms with field noise:

$$A_{real} = A_{synthetic} + Noise\ . \quad \text{(S2)}$$

The noisy synthetic waveforms are normalized trace by trace before entering the reconstruction and location workflow.

References

Staněk, F., Eisner, L., & Jan Moser, T. (2014). Stability of source mechanisms inverted from P-wave amplitude microseismic monitoring data acquired at the surface: Stability of source mechanisms inverted from P-wave amplitude data. *Geophysical Prospecting*, *62*(3), 475–490. https://doi.org/10.1111/1365-2478.12107

Figure S1. Number of traces in different apertures

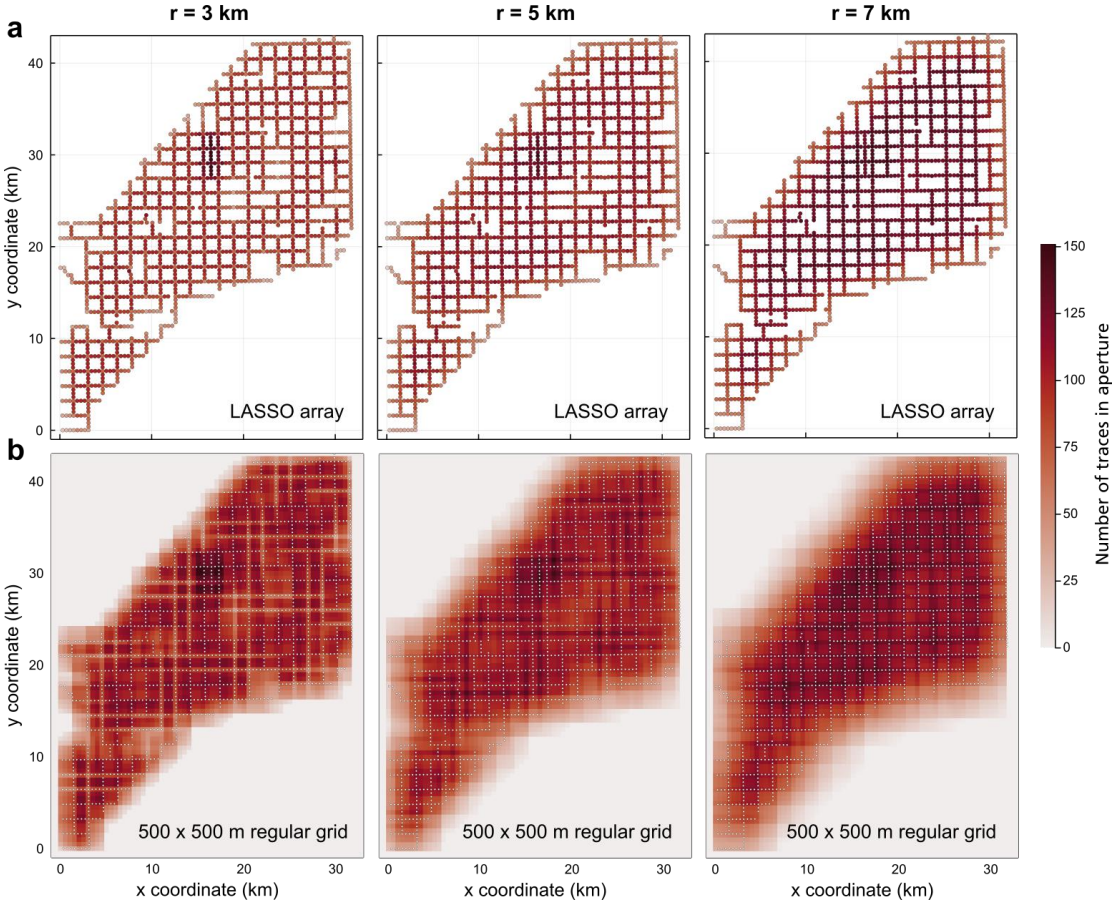

Figure S2. Coherence of the four field events using different apertures

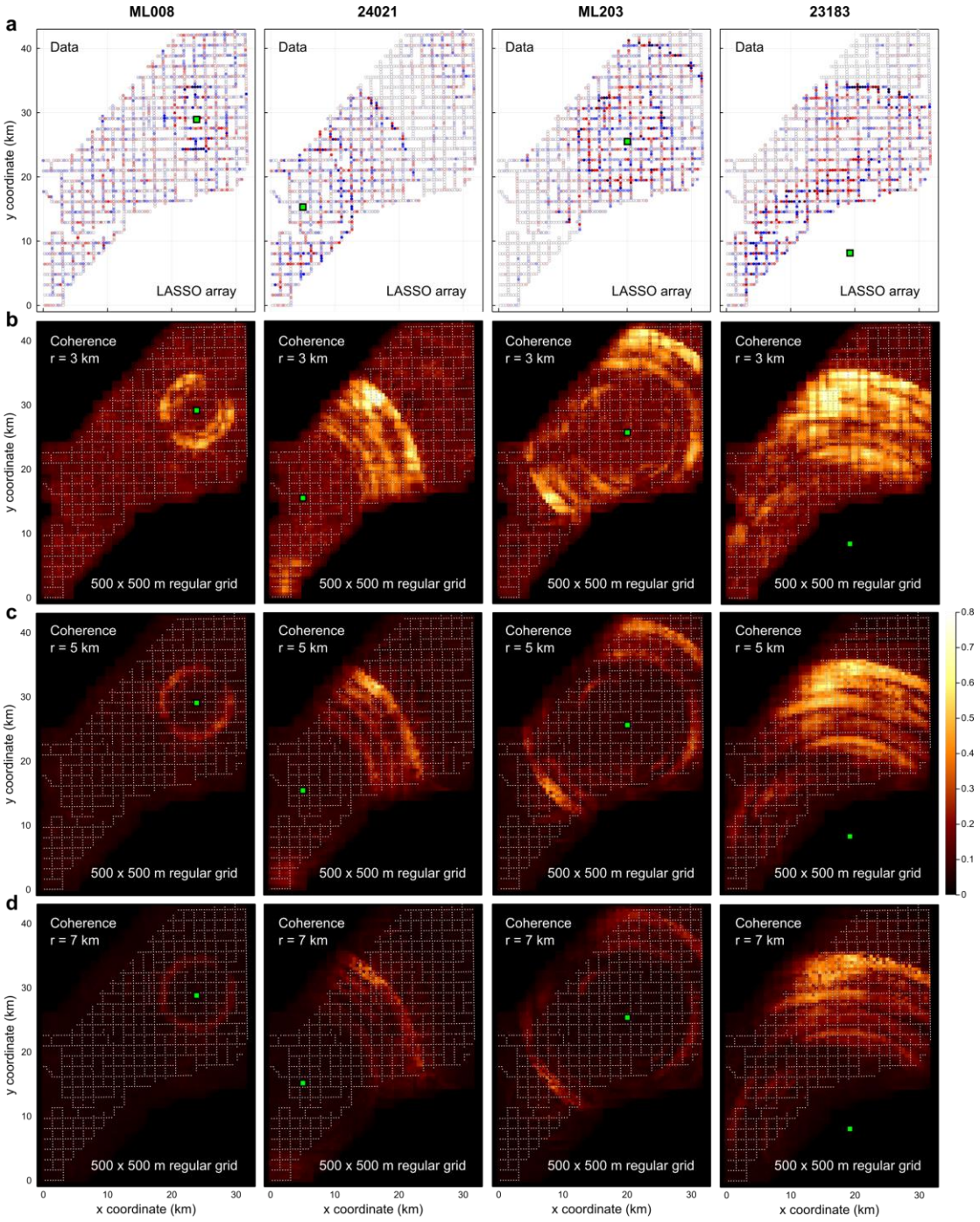

Figure S3. Reconstructed wavefields of the four field events using different apertures

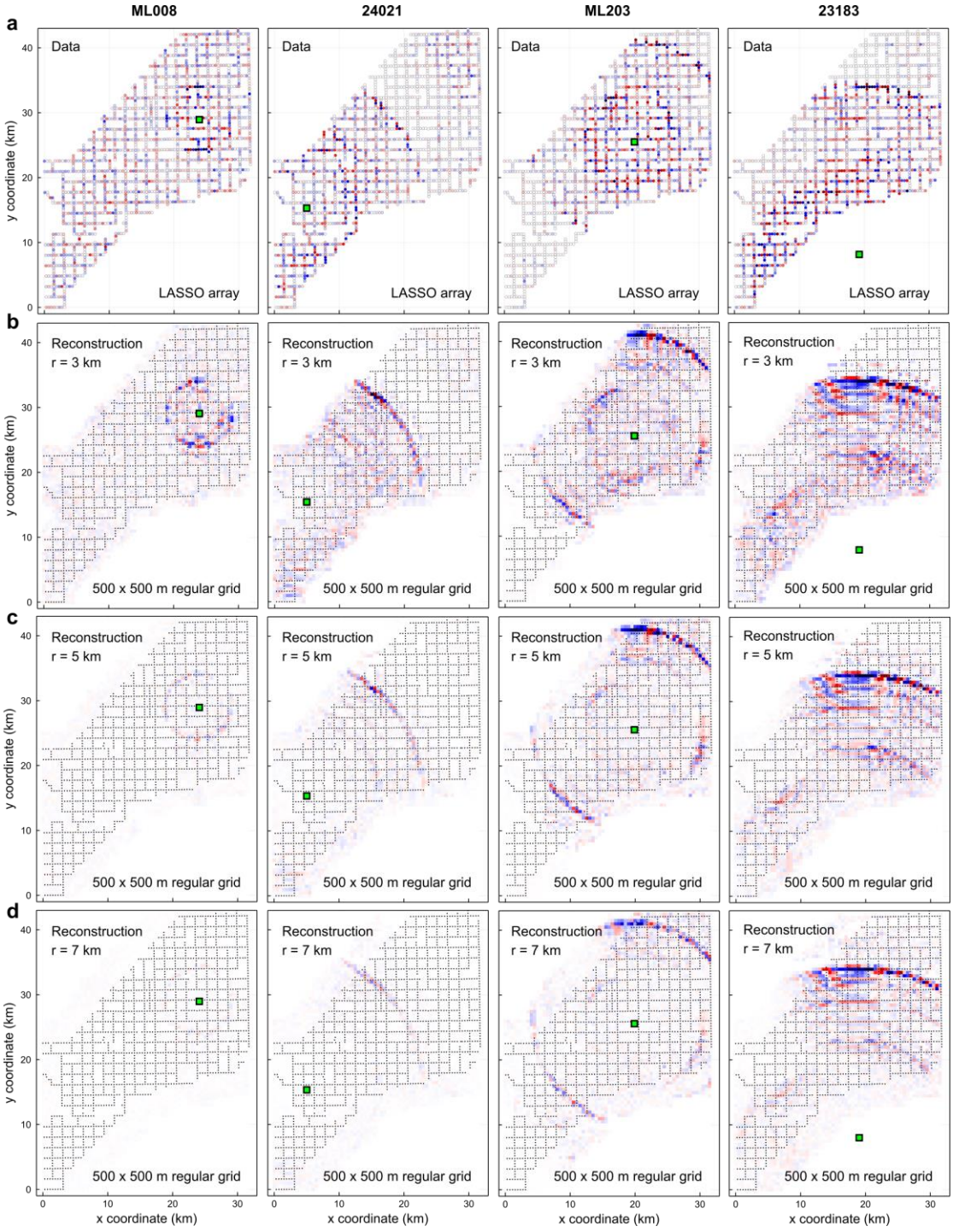

Figure S4. Unreconstructed and reconstructed waveforms of the four field events. (a) event ML008, (b) event 24021, (c) event ML203, (d) event 23183. The left column corresponds to raw traces of unreconstructed waveforms, and the right column are those of reconstructed waveforms. Only portions (50 traces) of the seismograms are shown.

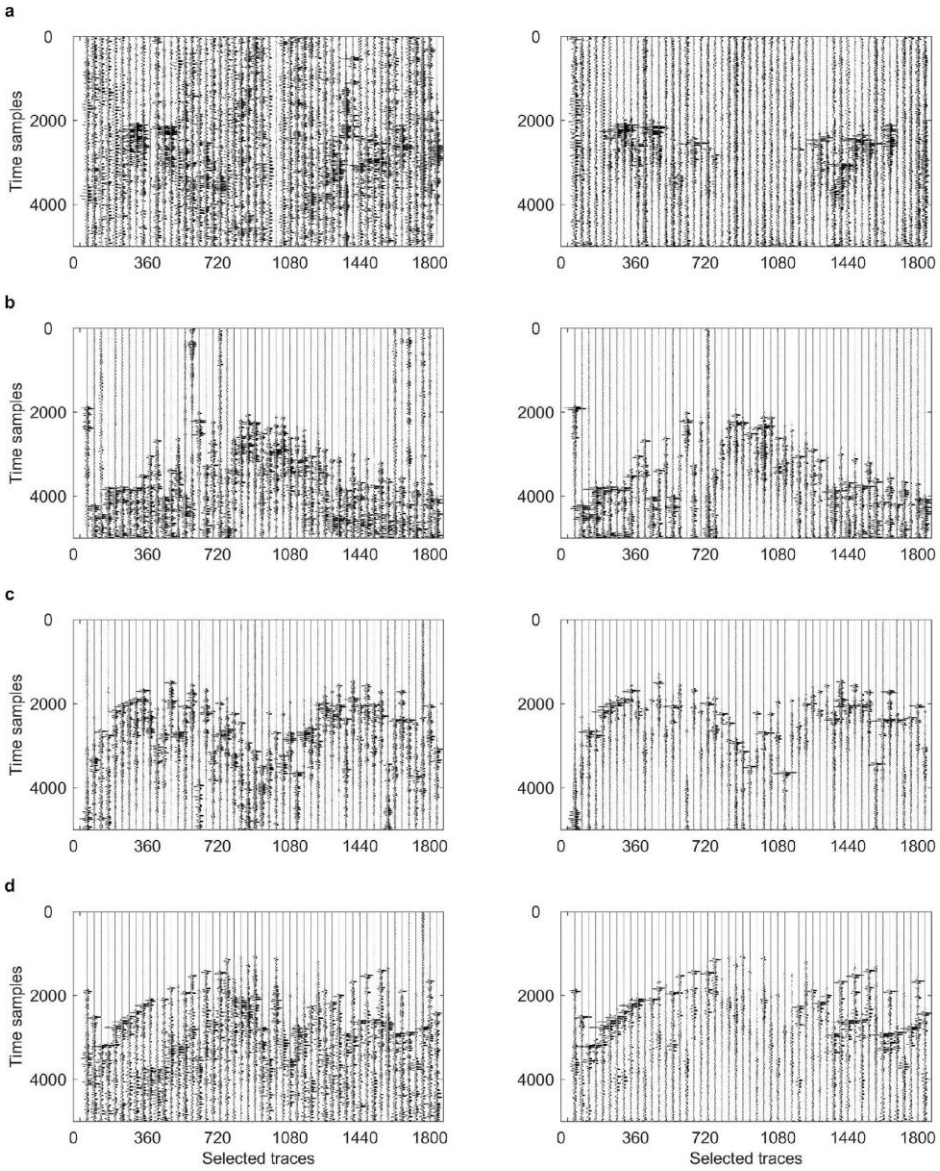

Figure S5. STA/LTA traces of the unreconstructed raw waveforms and reconstructed waveforms of the synthetic and field event ML203. The left column corresponds to STA/LTA traces of unreconstructed waveforms, and the right column are those of reconstructed waveforms. (a) to (c) correspond to different noise levels, (d) corresponds to the field event ML203. Only portions (about 50 traces) of the seismograms are shown.

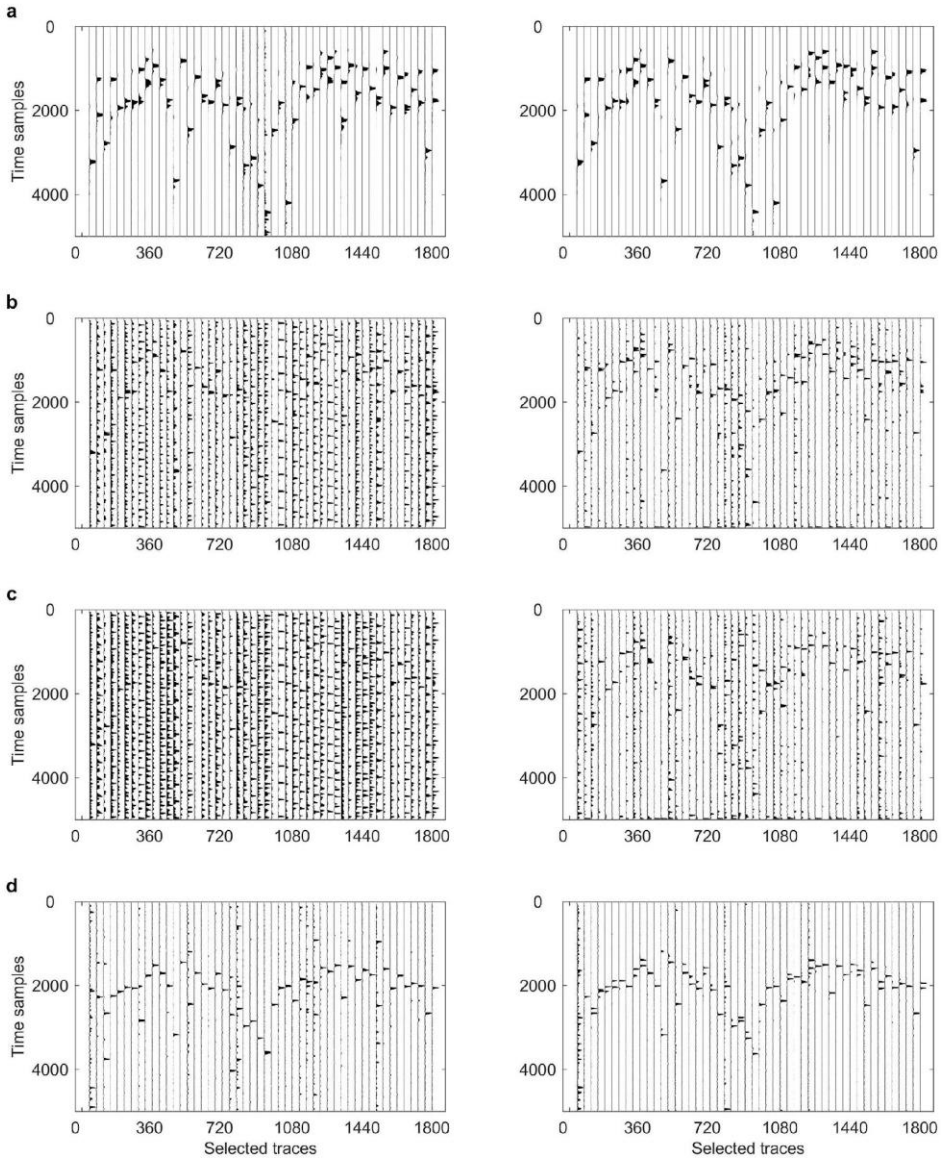

Figure S6. The source imaging results for the four field events using raw traces. (a) event ML008, (b) event 24021, (c) event ML203, (d) event 23183. The left column corresponds to the result of unreconstructed waveforms, and the right column images result from reconstructed waveforms. Reference locations from the catalog and/or previous studies are indicated as white circles. Please note the degradation of the depth resolution of event 24021 and event 23183, mainly caused by the array geometry and the properties of the chosen stacking operator. The horizontal resolution of the images, on the other hand, remains consistently high.

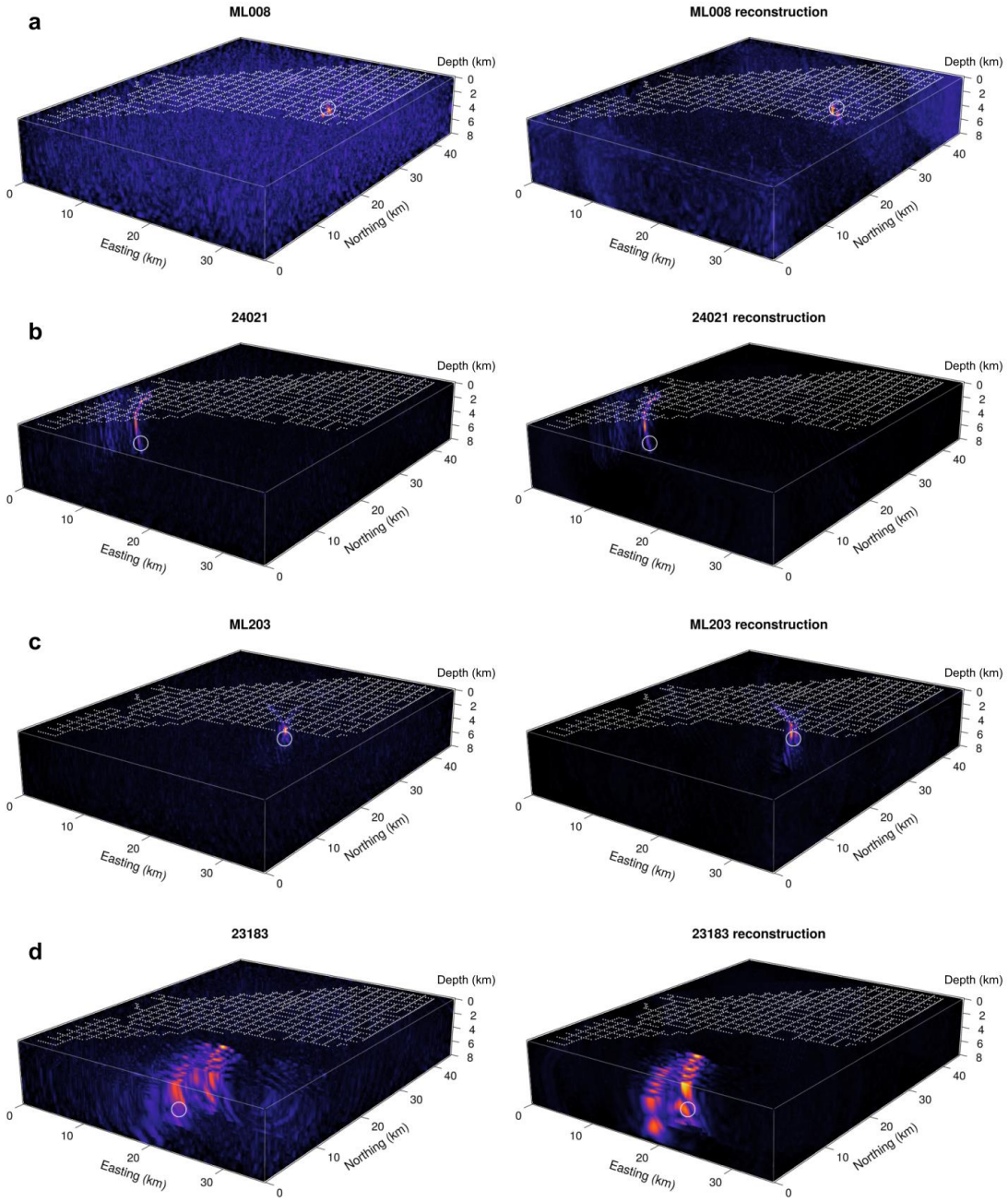

Figure S7. The source imaging results for the four field events using STA/LTA traces. (a) event ML008, (b) event 24021, (c) event ML203, (d) event 23183. The left column corresponds to the result of unreconstructed waveforms, and the right column images result from reconstructed waveforms. Reference locations from the catalog and/or previous studies are indicated by a circle.

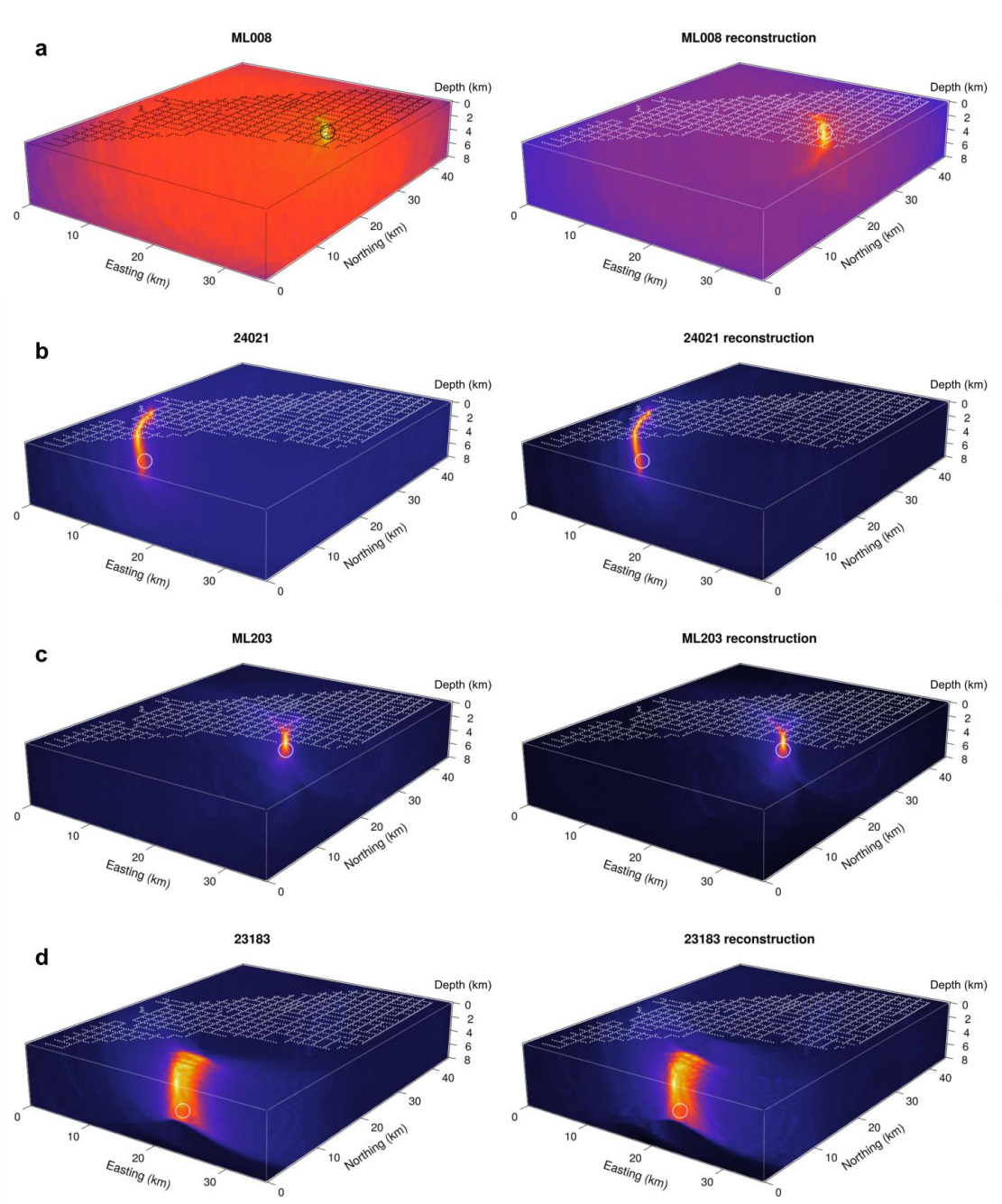

Movies S1 to S5: Synchronized animations of the raw data (left), its reconstruction (center) and the estimated waveform coherence (right) for the four field events and the synthetic event ML203 (SNR<1).